Editors' Suggestion | Featured in Physics

Evidence for Quasicritical Brain Dynamics

Leandro J. Fosque,[1,*] Rashid V. Williams-García,[2,†] John M. Beggs,[1,‡] and Gerardo Ortiz[1,§]
[1]Department of Physics, Indiana University, Bloomington, Indiana 47405, USA
[2]Department of Mathematical Sciences, Indiana University-Purdue University, Indianapolis, Indiana 46202, USA

(Received 1 September 2020; revised 20 November 2020; accepted 23 December 2020; published 1 March 2021)

Much evidence seems to suggest the cortex operates near a critical point, yet a single set of exponents defining its universality class has not been found. In fact, when critical exponents are estimated from data, they widely differ across species, individuals of the same species, and even over time, or depending on stimulus. Interestingly, these exponents still approximately hold to a dynamical scaling relation. Here we show that the theory of quasicriticality, an organizing principle for brain dynamics, can account for this paradoxical situation. As external stimuli drive the cortex, quasicriticality predicts a departure from criticality along a Widom line with exponents that decrease in absolute value, while still holding approximately to a dynamical scaling relation. We use simulations and experimental data to confirm these predictions and describe new ones that could be tested soon.

并不是准确的临界行为，而可以认为是一种准临界形态，可以解释这种测量评估变异性。

DOI: 10.1103/PhysRevLett.126.098101

Introduction.—A cubic millimeter of cortex is showered with approximately 10^5 synaptic inputs every second, even during sleep. The rate at which these synaptic currents arrive changes constantly, depending on cognitive state. This situation drastically constrains any statistical analysis of living cortical networks. While equilibrium approaches might serve as approximations, nonequilibrium methods are required to accurately describe its dynamics [1]. Yet even the nonequilibrium framework of self-organized criticality [2,3], often invoked in these studies [4,5], requires separation of timescales between a single incoming stimulus and the relaxation of the consequent avalanche. Such separation is not realistic in actual networks [6–8].

What is needed is an organizing principle for cortex dynamics that describes how these networks can appear to show some signatures of criticality despite receiving constantly changing external drive [9]. Work in Ref. [10] recorded from turtle visual cortex while movies with changing images were delivered to the retina; work in Ref. [11] recorded from freely moving and resting rats with changing levels of activity. In both studies, neuronal avalanches produced seemingly power law distributions with exponents that approximately followed a scaling relation [12,13], indicating closeness to criticality.

But what is perhaps most intriguing is that the exponents did not reveal a single universality class. Rather, the exponents could change across individuals, and even across time within an individual, all while approximately holding to a dynamical scaling relation. The data would seem to be at odds with the longstanding concept of a universality class [14].

Here, we address this apparent paradox with the principle of quasicriticality [7], which hypothesized that a healthy cortex always adapts to operate near a line of maximal dynamical susceptibility, and will be critical only in the limit of no external drive (stimulus, noise, or dissipation). It predicts that for nonzero drive, quantities like the dynamical susceptibility and information transmission will no longer display singularities. As drive increases, moving away from the critical point, the height of these peaks will decrease. Moving in parameter space along the (Widom) line of these maximal, but decreasing peaks, the avalanche (effective) exponents for size and duration as well as the branching ratio will decrease in testable ways (Fig. 3). The quasicritical region is defined by the domain in parameter space surrounding the Widom line [7]. As the cortex moves along the Widom line of optimality, it also will remain *close* to the critical point, so adherence to a scaling relation is expected. Using these predictions, we will show that quasicriticality can account for the pattern of data seen in recent experiments [11] without resorting to multiple universality classes. In addition, we show that our own experimental data fulfill quasicriticality's specific predictions (Fig. 3).

Critical vs quasicritical vs noncritical.—It is important to highlight physical distinctions between the various hypotheses. In neural activity data taken from cortical tissue, critical behavior can, in principle, be identified by examining dynamical scaling relations [14]. Power-law scaling permeates complex systems and a plethora of physical mechanisms generate scaling. In brain dynamics we argued [7] that the relevant nonequilibrium scaling is associated to the well-known *absorbing-state phase transitions*, the most important class of which is directed percolation [15]. The finite-size scaling assumption for probability distributions of avalanches at criticality, $P(q, L) = q^{-\tau_q}\Psi_q(q/L^{d_q})$,

 © 2021 American Physical Society

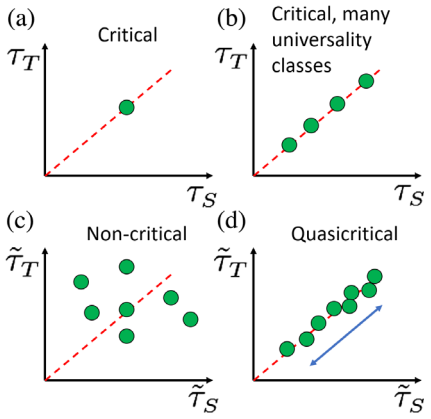

FIG. 1. Exponent relations and dynamical scaling line, of slope γ, for the various physical hypotheses (see text).

establishes relations between the critical exponents τ_q and fractional dimension d_q, for quantities q (e.g., avalanche size S and duration T) given a system of linear size L, where Ψ_q is the scaling function [14]. Assuming avalanches' size and duration satisfy scaling, then the conditional probability $P(S|T) \propto \delta(S - T^{\gamma})$. This, in turn, leads to the conditional expectation value $\overline{\langle S \rangle} \propto T^{\gamma}$ with a resulting scaling relation $\gamma = (\tau_T - 1)/(\tau_S - 1)$, where exponents τ_T and τ_S are from avalanche duration and size distributions, respectively [15]. A pair (τ_S, τ_T) defines a universality class [16] [see Fig. 1(a)]. The criticality hypothesis of brain dynamics argues for such fine-tuning behavior. Moreover, from scaling one obtains bounds on critical exponents. For instance, the average avalanche size $\langle S \rangle \propto L^{\sigma_S}$ with $\sigma_S = d_S(2 - \tau_S)$ if $\tau_S < 2$, meaning that $\langle S \rangle$ diverges with system size, while $\sigma_S = 0$ if $\tau_S > 2$.

Figure 1(b) depicts multiple universality classes; there are several pairs of exponents, each dot fixed on the line [17]. If the data were not critical, pairs of exponents might be observed, but they would not generally adhere to the scaling relation [Fig. 1(c)]. However, quasicriticality [Fig. 1(d)] predicts multiple pairs of exponents could be observed, all adhering to the scaling relation, and possibly moving along the line over time. Therefore, even though a system ideally belongs to a given universality class (τ_S, τ_T) [16], the *measured effective* exponents $\tilde{\tau}_q$ may vary as a function of the stimulus or noise. A natural question is, how do these effective exponents change as a result and how far from the dynamical scaling line do they lie? This is a subject we explore next.

Cortical branching model (CBM).—To address the question above we start analyzing the CBM [7]. This is a nonequilibrium stochastic cellular automaton that captures main features of neural network data. Since we are interested in robust generic phenomena we need a flexible platform such as the CBM to answer that question. Certainly, the topology of the network dictates universality and the nature of the phases involved in its phase diagram. For our purposes, we focus on the case of strongly connected graphs, i.e., those with irreducible adjacency matrices [18]. In that case, we uncovered a rich phase diagram including a normal region with subcritical and supercritical phases separated by a critical (or crossover) region, and a quasiperiodic (chaotic) phase. Critical exponents were analytically determined using mean-field approximations and found to coincide with (mean-field) directed percolation universality class. Determining the universality class of the CBM in a strongly connected graph is an interesting question beyond the scope of this work [19]. For more details we refer the reader to the original work [7].

TABLE I. Effective critical exponents for avalanche size and duration distributions as a function of τ_r and p_s.

τ_r	p_s	κ_w	$\tilde{\tau}_S$	$\tilde{\tau}_T$	$(\tilde{\tau}_T - 1)/(\tilde{\tau}_S - 1)$	γ
1	10^{-3}	1.10	1.57(1)	1.82(1)	1.44(3)	1.51(5)
1	10^{-4}	1.12	1.64(2)	1.99(4)	1.55(8)	1.57(3)
1	10^{-5}	1.17	1.69(2)	2.14(15)	1.65(22)	1.66(1)
5	10^{-3}	1.19	1.62(2)	1.85(8)	1.37(14)	1.37(3)
5	10^{-4}	1.23	1.67(1)	1.99(12)	1.48(18)	1.50(8)

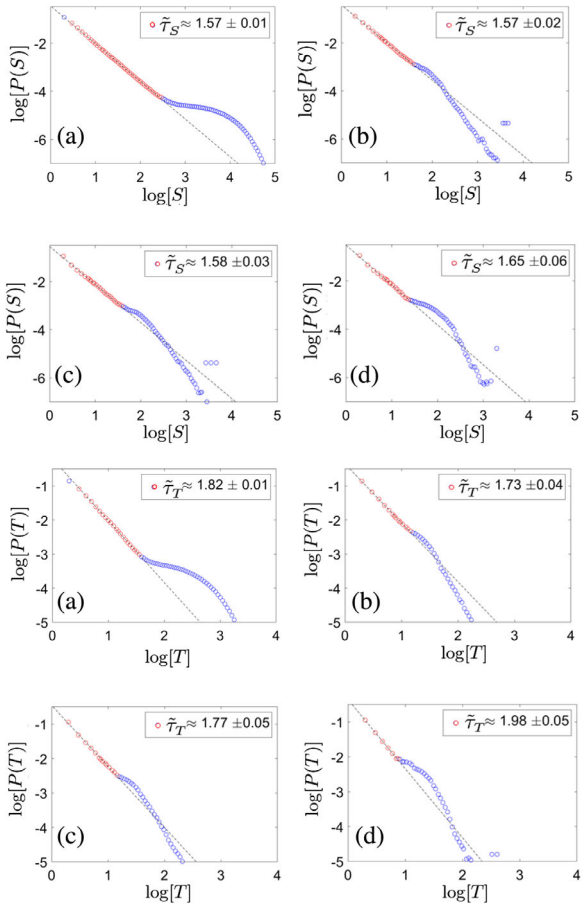

FIG. 2. Logarithmically binned avalanche size, and duration, probability distributions [22] for (a) CBM simulation with $p_s = 10^{-3}$, (b) Mouse data 23, (c) Mouse data 18, (d) rat data. Red circles were selected for fitting.

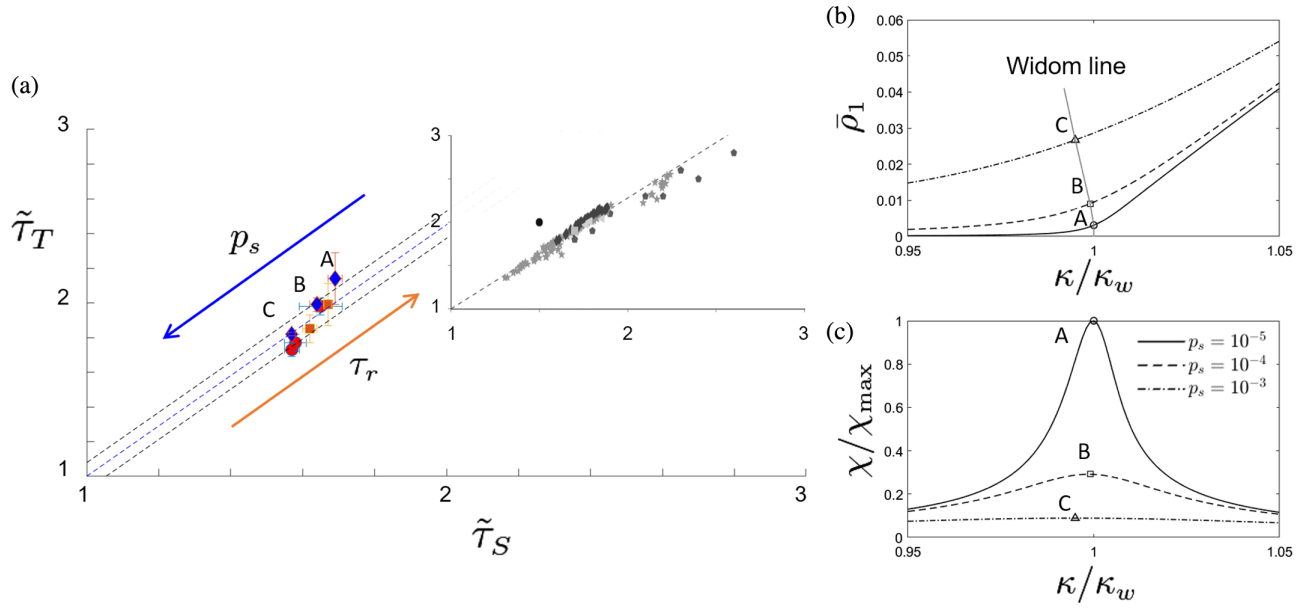

FIG. 3. Predictions of quasicriticality. (a) Simulations and data follow the scaling relation as predicted by quasicriticality. As p_s is increased (blue arrow) exponents $(\tilde{\tau}_T,\tilde{\tau}_S)$ decrease in the model (blue diamonds for $p_s = 10^{-5}, 10^{-4}, 10^{-3}$) while still approximately holding to the scaling relation (dashed line). Note that susceptibility curves A, B, and C in panel (c) correspond to these p_s values. Increasing τ_r (orange arrow) increases the magnitude of the effective exponents (the orange squares correspond to $\tau_r = 5$ for $p_s = 10^{-3}$ and 10^{-4}, respectively). Actual datasets (red circles) also lie near the line, and have reduced values of susceptibility and branching ratio κ_w, in agreement with the simulations. Our scaling line has a slope of 1.45(4), in agreement with our data and differs from the slope in Ref. [11] shown in the inset. Note that model parameters can be easily changed to match any slope, but that the trends in susceptibility and κ_w as p_s is increased will not change and constitute the specific predictions of the theory tested here. (b) Phase diagram showing how increased external drive leads to the Widom line; the y axis is the (time-averaged) density of active nodes (order parameter), the x axis is the branching ratio, κ (control parameter). With minimal external drive ($p_s = 10^{-5}$), the solid black line at A comes near the critical point. As the external drive is increased ($p_s = 10^{-4}$), the dashed line follows the solid black line, but rises above the critical point, with a gradual bend in the curve at B. Further increases in the external drive ($p_s = 10^{-3}$) cause the curve to rise more, bending near C. The thin gray line connecting A, B, C is the Widom line. Note that it tilts to the left, predicting that κ_w should decrease as p_s increases. (c) Susceptibility is maximal, but not divergent, along this line. Three plots of the susceptibility produced by simulations with different values of p_s. Note that increases in p_s cause peak susceptibility to decline, leading to flattened curves.

We analyze the region in parameter space close to the Widom line, representing the crossover domain where the dynamical susceptibility associated with the density of active nodes (order parameter) attains its largest values. We consider random, strongly connected, networks of $L = 128$ nodes, with a fixed in-degree of $k_{\text{in}} = 3$, branching parameter κ, with an exponential distribution of connection strengths [18].

In the CBM the magnitude of the input activity to the network is represented by a probability of spontaneous activation p_s. The refractory period τ_r, i.e., the number of time steps following activation during which a node cannot be made to activate, is a competing timescale in the problem.

As mentioned above, we want to explore the dynamical response in the domain surrounding the Widom line. To this end, for given values of p_s and τ_r, we locate the corresponding point along the Widom line by varying κ until the dynamical susceptibility, at κ_w, becomes maximal. It is precisely for this set of parameters that we next determine the effective exponents $(\tilde{\tau}_S, \tilde{\tau}_T)$ for avalanche size and duration distributions. Let us start by fixing $\tau_r = 1$ and vary p_s in the range $p_s \in [10^{-5}, 10^{-3}]$. The effective exponents, together with the computed values of κ_w, are shown in Table I. As one can see, as p_s increases, the exponents decrease in magnitude. Increasing the probability of spontaneous activity p_s, increases activity and, therefore, produces positive interference with avalanches, increasing their size and duration accordingly. At the same time, this induces a smaller magnitude of the effective exponents. Consider next increasing the refractory period to $\tau_r = 5$. As appreciated in Table I, the optimal κ_w is shifted to larger values. By increasing τ_r, one reduces the number of possible nodes that could become active, which in turn reduces the size of the avalanches lowering the probability for the avalanche to continue spreading, and increases the magnitude of the effective exponents. These constitute testable predictions of quasicriticality which could be checked, for instance, by application of drugs in living tissue resulting in an increase of the average refractory period.

Several comments are in order. First, although one could in principle establish a finite-size scaling extrapolation to

$L \to \infty$ [18], these effective exponents will never represent exact critical exponents since the system, when $p_s \neq 0$, is not scale invariant. Nonetheless, the effective exponents move along the dynamical scaling line. The universality class (τ_S, τ_T), when $p_s \to 0$, is unique [19] but depending on physical conditions the measured effective exponents wander along the dynamical scaling line. Second, the behavior just derived from computation corresponds to the optimal situation, that is, when the system operates exactly at the Widom line. On this line, one should obtain the best numerical agreement between the slope γ derived from the effective exponents and the one obtained from the conditional expectation value $\overline{\langle S \rangle}$. Finally, as long as the system is close to the Widom line, that is, the quasicritical region [7], one will arrive at the same conclusions. But what happens if the system operates very far from the optimal region, such as in the deep subcritical region [18]?

Signs of quasicriticality in experimental data.—Before testing the quasicriticality hypothesis with empirical data, we need to make careful assumptions and apply strict criteria [18]. First, because living neural networks are open nonequilibrium systems, their state will fluctuate in two ways: (i) due to the inherent noise of external dynamic inputs and (ii) the systematic fluctuations of the network response to those inputs. The result is fluctuations of the network state about a moving average in a multidimensional state space. This is realized, not only by dynamic external inputs, but also by the physiological responses of the network to those inputs, e.g., synaptic plasticity. In terms of the CBM, this means that the spontaneous activation probability p_s and the branching parameter κ will be dynamic—a situation not considered in our simulations.

According to our theory, however, fluctuations of the empirical values of p_s and the branching ratio σ (which we use as a proxy for the κ) induce fluctuations in the values of the effective critical exponents and hence the *apparent* universality class. Within a sufficiently short time frame, state fluctuations will be minimal; it is under these conditions that the network state can best be characterized as sub-, quasi-, or super-critical. Second, in order to satisfy quasicritical scaling, empirical data must be taken from or near the peak of maximum susceptibility, i.e., the quasicritical state [7].

A reliable method is then needed to quantify neural network state fluctuations, bin the data to adjust the time frame, and finally characterize the data. We start by quantifying these fluctuations in the language of statistical physics, introducing the local time fluctuation (LTF) of the network state. With a neural network of size L, we write the density of active nodes at time t as $\rho_1(t) = (1/L)\sum_{i=1}^{L} \delta_{z_i(t),1}$, where $z_i \in \{0, 1\}$ represents the state of quiescence or spiking, respectively, for neuron i. The mean population firing rate over a short time frame of ΔT time steps is then $\langle \rho_1(t) \rangle_t = (1/\Delta T)\sum_{t=1}^{\Delta T} \rho_1(t)$. The variability of $\rho_1(t)$ is the dynamical susceptibility [7], $\chi = L[\langle \rho_1^2(t) \rangle_t - \langle \rho_1(t) \rangle_t^2]$. Because χ varies dramatically depending on L, we normalize by the number of neurons to define the LTF $= (1/\langle \rho_1(t) \rangle_t)\sqrt{\chi/L}$. Effective exponents are then calculated from bins with similar, intermediate LTF values [18]. Alternatively, calculating σ and χ for each bin and mapping to LTF values shows that its intermediate values correspond to maxima of χ and intermediate values of σ. This is consistent with predictions made by our theory.

TABLE II. Effective exponents from empirical data. Sets (1) and (2) correspond to mouse cortical culture data and (3) corresponds to rat data.

Set	χ	σ	$\tilde{\tau}_S$	$\tilde{\tau}_T$	$(\tilde{\tau}_T - 1)/(\tilde{\tau}_S - 1)$	γ
1	0.0096	0.7101	1.57(2)	1.73(4)	1.29(3)	1.33(1)
2	0.019	0.7322	1.58(3)	1.77(5)	1.33(5)	1.33(2)
3	0.0475	0.7433	1.65(6)	1.98(5)	1.50(6)	1.48(7)

We analyze the dense microelectrode array recordings from rodent cortical tissue that were publicly posted on the CRCNS website [20,21]. For selection of specific datasets, we required a bump in the avalanche distributions when the data were in the supercritical regime (larger bins) and no bump when in the subcritical regime (smaller bins; see Fig. 2). Although many datasets were consistent with quasicriticality, here we present only the 3 sets that satisfied these stringent criteria (for a clear description of all criteria involved in the analysis see the Supplemental Material [18]). Table II lists results from the three datasets, along with values of the effective exponents. Datasets (1) and (2) are from mouse organotypic cortical cultures with number of neurons $L = 310$ and $L = 180$, respectively, binned at 1 ms. Dataset (3) is from a rat organotypic cortical culture with $L = 107$ and is binned at 5 ms. Although the rest of the datasets did not satisfy the stringent criteria, nonetheless, the determined effective exponents lie along the scaling line [18].

In agreement with our predictions, the values of χ and σ from the data grow with the effective exponents. We report here branching ratios estimated from dividing the number of descendant neurons by the number of ancestor neurons. We found more advanced methods [23] produced the same trends, but with smaller differences. Our experimental data (together with data from Ref. [11]) and theoretical simulations are summarized in Fig. 3.

Outlook.—We have shown that quasicriticality can explain why cortical networks do not produce a single set of characteristic exponents as expected from a universality class. External inputs force these networks to operate in nonequilibrium conditions, away from a critical point. Yet the exponents produced under varying conditions still satisfy a scaling relation, indicating closeness to criticality. Quasicriticality predicts that increased drive will force cortical networks to depart from criticality, near the Widom line, preserving maximal susceptibility and

information transmission. Moving along this line as drive is increased, the branching ratio at maximal susceptibility will decrease, and susceptibility will decrease. Simulations predict this, and the best datasets we have are consistent with these predictions.

Future experiments must causally manipulate external drive, carefully tracking how the branching ratio and the susceptibility respond. These experiments have the potential to refute quasicriticality, or to further strengthen its standing.

J. M. B. gratefully acknowledges support from NSF Grant No. 1513779 and Indiana University Bridge funds.

L. J. F. and R. V. W-G. contributed equally to this Letter.

*lfosque@iu.edu
†rwgarcia@iupui.edu
‡jmbeggs@indiana.edu
§ortizg@indiana.edu

[1] J. A. Bonachela, S. De Franciscis, J. J. Torres, and M. A. Muñoz, Self-organization without conservation: are neuronal avalanches generically critical?, J. Stat. Mech. (2010) P02015.
[2] P. Bak, C. Tang, and K. Wiesenfeld, Self-Organized Criticality: An Explanation of the $1/f$ Noise, Phys. Rev. Lett. **59**, 381 (1987).
[3] H. J. Jensen, *Self-Organized Criticality: Emergent Complex Behavior in Physical and Biological Systems* (Cambridge University Press, New York, 1998).
[4] C. W. Eurich, J. M. Herrmann, and U. A. Ernst, Finite-size effects of avalanche dynamics, Phys. Rev. E **66**, 066137 (2002).
[5] A. Levina, J. M. Herrmann, and T. Geisel, Phase Transitions towards Criticality in a Neural System with Adaptive Interactions, Phys. Rev. Lett. **102**, 118110 (2009).
[6] V. Priesemann, M. Wibral, M. Valderrama, R. Pröpper, M. Le Van Quyen, T. Geisel, J. Triesch, D. Nikolić, and M. H. J. Munk, Spike avalanches in vivo suggest a driven, slightly subcritical brain state, Front. Syst. Neurosci. **8**, 108 (2014).
[7] R. V. Williams-García, M. Moore, J. M. Beggs, and G. Ortiz, Quasicritical brain dynamics on a nonequilibrium Widom line, Phys. Rev. E **90**, 062714 (2014).
[8] R. V. Williams-García, J. M. Beggs, and G. Ortiz, Unveiling causal activity of complex networks, Europhys. Lett. **119**, 18003 (2017).
[9] V. Priesemann and O. Shriki, Can a time varying external drive give rise to apparent criticality in neural systems?, PLoS Comput. Biol. **14**, e1006081 (2018).
[10] W. L. Shew, W. P. Clawson, J. Pobst, Y. Karimipanah, N. C. Wright, and R. Wessel, Adaptation to sensory input tunes visual cortex to criticality, Nat. Phys. **11**, 659 (2015).
[11] A. J. Fontenele *et al.*, Criticality between Cortical States, Phys. Rev. Lett. **122**, 208101 (2019).
[12] J. P. Sethna, K. A. Dahmen, and C. R. Myers, Crackling noise, Nature (London) **410**, 242 (2001).
[13] S. Papanikolaou, F. Bohn, R. L. Sommer, G. Durin, S. Zapperi, and J. P. Sethna, Universality beyond power laws and the average avalanche shape, Nat. Phys. **7**, 316 (2011).
[14] H. Nishimori and G. Ortiz, *Elements of Phase Transitions and Critical Phenomena* (Oxford University Press, Oxford, 2011).
[15] M. Henkel, H. Hinrichsen, and S. Lübeck, *Non-Equilibrium Phase Transitions* (Springer Verlag, Dordrecht, 2008), Vol. I and II.
[16] Technically, in this case, one needs additional independent exponents to uniquely define the universality class together with its corresponding scaling relation.
[17] M. Yaghoubi, T. de Graaf, J. G. Orlandi, F. Girotto, M. A. Colicos, and J. Davidsen, Neuronal avalanche dynamics indicates different universality classes in neuronal cultures, Sci. Rep. **8**, 3417 (2018).
[18] See Supplemental Material at http://link.aps.org/supplemental/10.1103/PhysRevLett.126.098101 for describing aspects of the simulation and statistical analysis of experimental datasets, including an example study of finite size scaling.
[19] Strong heterogeneity in networks may be relevant to scaling, in particular, strong rare fluctuations may even lead to a smearing of the transition. For a discussion on the potential emergence of Griffiths phases in those cases see M. A. Muñoz, R. Juhász, C. Castellano, and G. Ódor, Griffiths Phases on Complex Networks, Phys. Rev. Lett. **105**, 128701 (2010); G. Ódor, Robustness of Griffiths effects in homeostatic connectome models, Phys. Rev. E **99**, 012113 (2019).
[20] S. Ito, F. C. Yeh, N. M. Timme, P. Hottowy, A. M. Litke, and J. M. Beggs (2016), CRCNS.org https://doi.org/10.6080/K07D2S2F.
[21] N. M. Timme, N. Marshall, N. Bennett, M. Ripp, E. Lautzenhiser, and J. M. Beggs (2016), CRCNS.org https://doi.org/10.6080/K0PC308P.
[22] K. Christensen and N. R. Moloney, *Complexity and Criticality* (Imperial College Press, London, 2005).
[23] J. Wilting and V. Priesemann, Inferring collective dynamical states from widely unobserved systems, Nat. Commun. **9**, 2325 (2018).